Selection rules for the double space group O1h

H. Kunert, J. Popenda, M. Suffczynski

Classification
Physics Abstracts
61.50E — 77.80

SELECTION RULES FOR THE DOUBLE SPACE GROUP O_h^1

H. KUNERT, J. POPENDA

Politechnika Poznanska, ul. Piotrowo 3, 60-965 Poznan, Poland

and M. SUFFCZYNSKI

Instytut Fizyki PAN, Al. Lotnikow 32/46, 02-668 Warszawa, Poland

(*Reçu le 25 novembre 1977, accepté le 19 janvier 1978*)

Résumé. — Les produits directs de représentations irréductibles du groupe double O_h^1 (groupe de symétrie de la structure cubique simple et de celles du chlorure de césium, des perovskites et du trioxyde de rhénium) sont réduits pour les quatre points de symétrie maximum de la zone de Brillouin.

Abstract. — The octahedral symmorphic space group O_h^1 is the symmetry group of the simple cubic. the caesium chloride. the perovskites and the rhenium trioxide structures. The direct products of irreducible representations of the double space group O_h^1 are reduced for the four points of highest symmetry of the Brillouin zone.

1. **Introduction.** — The first of the octahedral space groups, O_h^1 or Pm3m, the symmorphic group based on the simple cubic Bravais lattice, is the symmetry group of several different crystal structures. The first of these is the simple cubic structure in which there is one atom per unit cell.

The second, the caesium chloride structure, is represented by several ionic crystals, including CsCl, CsBr, CsI, RbCl, TlCl, TlBr, several compounds, such as CaB_6, Cu_3N, $AuCu_3$, numerous intermetallic binary compounds, like LiAg, AlNd, FeAl, FeTi, compounds of magnesium : MgAg, -Sr, -La, -Ce, -Pr, -Au, -Hg, -Tl, of beryllium : BeCo, -Cu, -Pd, of copper : CuZn and CuPd, of zinc : ZnAg, -La, -Ce, -Pr, -Au, of thallium : TlCa, -Sb, -I, -Bi.

The third, the perovskite structure, is the structure of numerous ternary compounds where the molecules contain a transition metal and three oxygen, fluorine, chlorine or bromine atoms, like : $NaNbO_3$, $NaTaO_3$, $NaWO_3$, $CaTiO_3$, $KTaO_3$, $SrTiO_3$, $BaTiO_3$, $CaZrO_3$, $CaSnO_3$, $SrZrO_3$, $SrSnO_3$, $SrCeO_3$, $PbTiO_3$, $BaZrO_3$, $PbZrO_3$, $LaAlO_3$, $LaKO_3$, $LaCrO_3$, $LaMnO_3$, $LaFeO_3$, $KMnF_3$, $KMgF_3$, $KNiF_3$, $KCdF_3$, $RbCaF_3$, $RbMnF_3$, $CsCaF_3$, $CsCdCl_3$, $CsCdBr_3$, $CsHgCl_3$, $CsHgBr_3$, also Mn_3SnN, and many others.

The group O_h^1 is also the space group of rhenium trioxide, ReO_3, a compound similar to perovskites. An extensive list of the crystals of symmetry O_h^1, together with the ionic radii, can be found in a report by Slater [1], who also derived the irreducible representations for this space group [2].

The simple cubic structure is the structure of α-Po below 10 °C [3]. Because of heating by alpha decay the temperature of polonium in surroundings at room temperature is about 75 °C, but there is considerable difficulty in estimating the exact temperature of the specimens examined by X-rays.

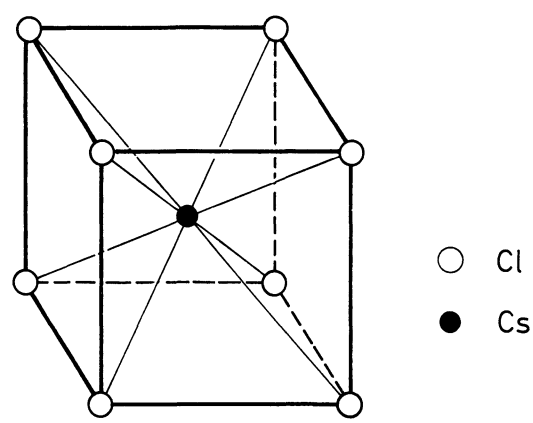

FIG. 1. — Unit cell for the caesium chloride structure.

The caesium chloride structure is shown in figure 1. There is a caesium atom at the origin (0, 0, 0) and chlorine at (1/2, 1/2, 1/2) *a*, where *a* is the lattice constant.

The cubic perovskite structure is shown in figure 2, for $SrTiO_3$. There is a titanium atom at the origin, oxygens at (1/2, 0, 0), (0, 1/2, 0), (0, 0, 1/2), Sr at (1/2, 1/2, 1/2), in units of the lattice constant *a*.

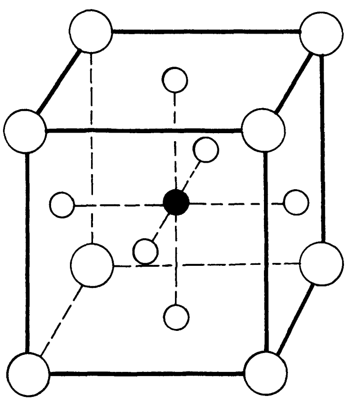

FIG. 2. — Unit cell for the cubic perovskite-type compound $SrTiO_3$.

ReO_3 contains a single rhenium atom per unit cell. The rhenium atom is situated at the origin, at a site with full cubic O_h symmetry. The oxygen atoms occupy positions at the face centres of the cubic cell, at sites with tetragonal D_{4h} point symmetry, see figure 3.

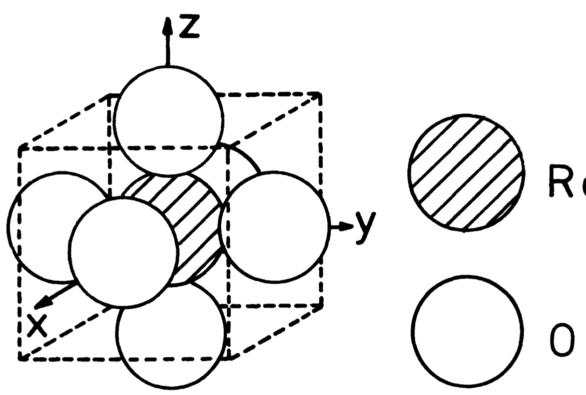

FIG. 3. — Unit cell for the ReO_3 structure. The Re atom is located at the origin, the O atoms occupy positions at the face centres.

The Brillouin zone for the space groups O_h^1, O_h^2, O_h^3, O_h^4 is simple cubic, and is shown in figure 4, with labels of Miller and Love (M-L) [4] for the symmetry points and lines. Characters of the irreducible representations of the wave vector groups for the space group O_h^1 were published by Bouckaert, Smoluchowski and Wigner [5], for the double group by Elliott [6], later by Zak *et al.* [7] and Bradley and Cracknell [8]. The irreducible representations for O_h^1 can be found in the tables of Kovalev [9], in the report of Slater [2], and in the tables of Miller and Love [4], whose labels of the irreducible representations we will use here.

Tovstyuk and Tarnavskaya [10] presented a general discussion, based on group theoretical arguments, of the energy spectrum in crystals with the octahedral symmetries O_h^1-O_h^{10}. References to the theoretical papers on the O_h^1 symmetries can be found in the monograph of Bradley and Cracknell [8].

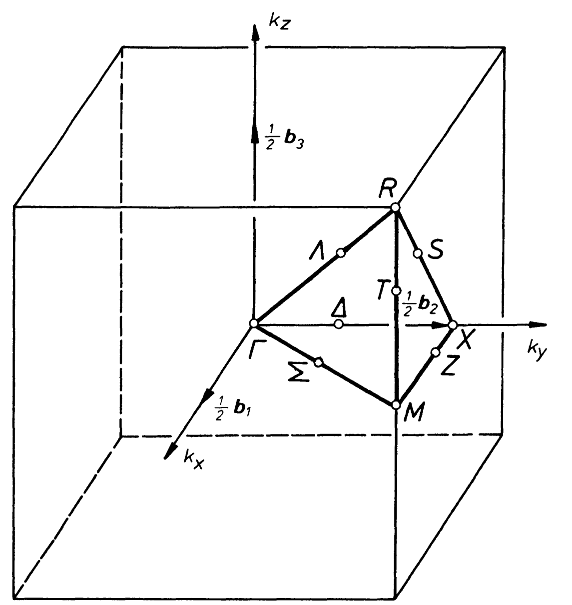

FIG. 4. — Brillouin zone for the simple cubic Bravais lattice.

2. **Caesium chloride structure.** — In CsCl type alkali halides a peculiar F-centre absorption structure has been observed at the fundamental absorption edge, strikingly different from the other alkali halides. The optical absorption band of F-centre in caesium halides at low temperatures has two or three components [11, 12]. A strong spin-orbit coupling can account for two components. After early attempts to explain the structure [13, 14], Moran [15] has shown that the F-centre absorption band in caesium halides can be explained by the instantaneous distortion of the F-centre environment from cubic symmetry induced by the motion of the bcc lattice. Agreement with experimental results for CsF, CsCl, CsBr and CsI has been achieved. The different relative strengths of the various cubic and noncubic interactions account for the striking contrast between a caesium halide F-centre and those observed in the salt crystals with a relatively light alkali metal [15].

Electronic energy bands have been labelled by the BSWE [5, 6] labels and calculated for CsI by Onodera [16] who found the direct gap at the Brillouin zone centre.

Electronic energy bands for TlCl and TlBr have been calculated [17-19], with the result that the direct gap is at the X point at the centre of the Brillouin zone face. This is found to be in agreement with recent results of the ultraviolet photoemission studies in TlCl [20].

The observed doublet structure of the first exciton transition in simple cubic TlCl [21] is explained as arising from Coulombic and exchange interactions, which lead to intra- and intervalley scattering between the excitons formed of electron-hole pairs at non-equivalent X-points of the Brillouin zone [22-24].

The band structure of caesium halides and rubidium chloride has been investigated theoretically and experimentally [25-34].

3. **Review of experimental work on perovskites.** — Numerous compounds with the perovskite type structure are of theoretical interest and significant practical importance because they possess ferroelectric, semiconducting or superconducting properties.

$KNiF_3$ perovskite crystals have been investigated by optical absorption studies and by nuclear magnetic resonance [35-37].

Recently structural phase transitions have been found to occur in perovskite compounds with phonon soft mode instabilities appearing at various symmetry points of the Brillouin zone. The phase transitions have been investigated in $KMnF_3$, $RbCaF_3$, $SrTiO_3$, $BaTiO_3$, $PbTiO_3$, $KTaO_3$, $CaPbCl_3$.

In particular, strontium titanate, $SrTiO_3$, and several other perovskite type compounds have been the subject of extensive studies mainly because of their ferroelectric properties with an expected Curie temperature in the range of helium temperatures [38].

It is believed that the high value of the dielectric constant of $SrTiO_3$ is mainly due to the optical phonon mode at the zone centre.

Unoki and Sakudo [39] with the help of their electron spin resonance measurements of Fe^{3+} ions in $SrTiO_3$ have demonstrated a phase transition at 110 K from the cubic perovskite symmetry O_h^1 to the tetragonal D_{4h}^{18} symmetry. This transition is not accompanied by any anomalies in the dielectric constant.

The X-ray study by Lytle [40] revealed a small tetragonal distortion below 110 K but the unit cell volume remains unchanged through the transition. The small tetragonal distortion manifests itself in the ESR experiments [41]. The most remarkable change at the transition was revealed however, by measurements of the elastic constants [42]. The interesting characteristic feature of this transition lies in its extremely small, below 1 promille, lattice distortion, indicative of a second order phase change, combined with other well defined anomalies (see Fig. 5).

Detailed inelastic neutron scattering experiments have shown that the 110 K transition is caused by a soft mode instability at the (111) zone boundary. A systematic investigation of the phonon spectrum was concentrated on the phonon branches near the zone centre as well the zone boundaries of high symmetry directions. The neutron scattering intensity distribution in the low temperature phase was found to be essentially in agreement with the Raman scattering measurements [43] and the crystal structure deduced from ESR experiments [39, 41].

Neutron inelastic scattering measurements in perovskite crystals such as $SrTiO_3$, $KMnF_3$, $LaAlO_3$, etc.

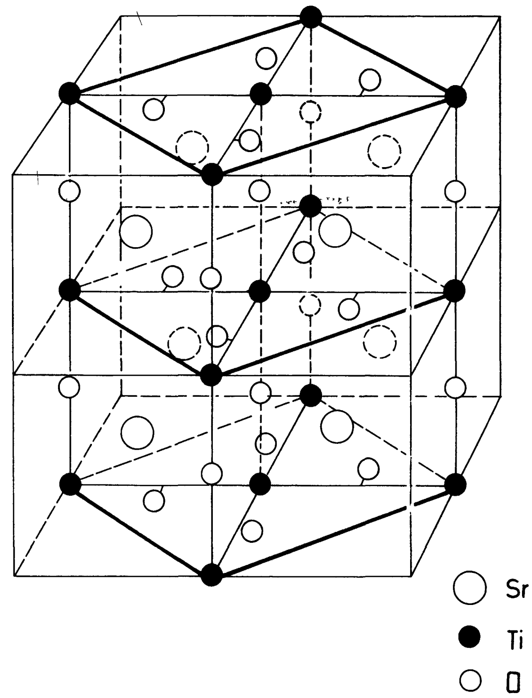

FIG. 5. — Unit cell for the tetragonal structure of $SrTiO_3$ with the D_{4h}^{18} space group. The cell contains four molecular units and its dimensions are $a\sqrt{2}$, $a\sqrt{2}$, $2c$, where a and c correspond to the tetragonal one molecular unit. The ratio $c/a = 1.000\,62$ at 4.2 K.

have been made by Cowley [44], Riste *et al.* [45, 46], Shirane *et al.* [38, 47-49], Töpler *et al.* [50], and others [51, 52]. The central peak has been observed [46, 50, 52]. The antiferrodistortive phase transition in $SrTiO_3$ at 105 K has been interpreted as due to the softening of the optical transverse Γ_{25} phonon at the Brillouin zone boundary R point [46, 50].

The linear thermal expansion coefficients for monodomain crystals of $SrTiO_3$, measured near the displacive phase transition at 106.8 K have been found to be different in the two perpendicular directions [53].

Neutron scattering studies of soft modes in the critical temperature region in cubic $BaTiO_3$ have been performed [54, 55].

Light scattering studies on the soft phonon phase transitions in $SrTiO_3$, $BaTiO_3$, etc. have been made [56, 57].

Fleury and Lazay [58, 59] measured the temperature dependence of the Brillouin scattering spectrum of $BaTiO_3$ in the room temperature phase.

Accumulating experimental studies of the soft modes in perovskites, particularly by inelastic photon and neutron scattering, or the soft mode spectroscopy, are reviewed inter alia by Scott [60].

In $KMnF_3$ [47-49] the zone boundary phonon dispersion branch extending from the R point to the M point is extremely soft, and the R phonon instability at 186 K [48] is followed by an M_3 phonon instability at 91.5 K [61].

$KMnF_3$ undergoes structural phase transitions : at 186 K from the O_h^1 (Pm3m) to D_{4h}^{18} (14/mcm) [48, 49] and at 91.5 K from D_{4h}^{18} to D_{4h}^5 (P4/mbm) symmetry [61, 62].

The related compounds K_2MnF_4 and Rb_2MnCl_4 have perovskite type layered structure with the D_{4h}^{17} (I4/mmm) symmorphic group symmetry [63, 64], (see Fig. 6).

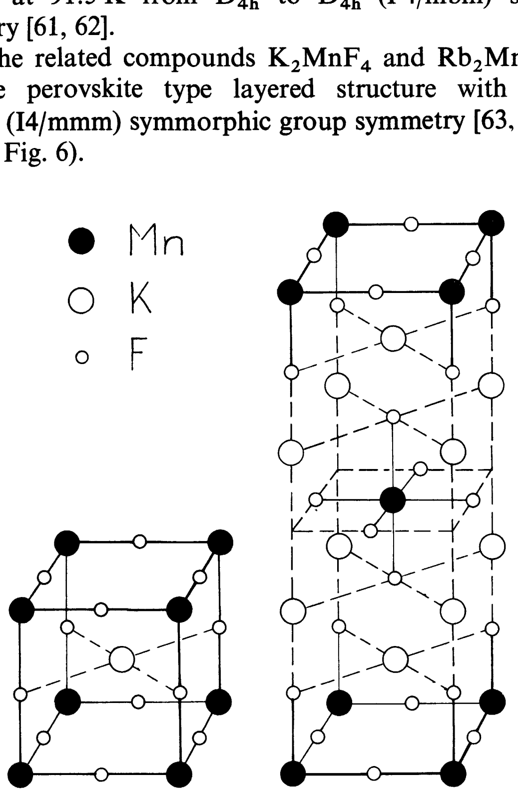

FIG. 6. — Unit cell for the cubic perovskite structure (space group O_h^1) of $KMnF_3$ with the lattice constant $a = 4.19$ Å, and for the perovskite-type layer tetragonal structure (D_{4h}^{17}) of K_2MnF_4 with $a = 4.22$ Å and $c = 13.38$ Å.

The Raman-active modes of symmetry $\Gamma_1^+(A_{1g})$ and $\Gamma_5^+(E_g)$ in tetragonal K_2MnF_4 and modes of symmetry X_1^+ and X_5^+ in cubic $KMnF_3$, respectively, have been considered [64].

EPR experiments on $RbCaF_3$ [65] have revealed the occurrence of structural phase transitions at low temperatures, and Raman scattering data [66] have shown that the transition at 200 K is similar to the cubic-tetragonal transition occurring in $SrTiO_3$ and $KMnF_3$ [65-68].

The observations in $RbCaF_3$ show an excellent correspondence with those in $KMnF_3$ and there are strong similarities with the $SrTiO_3$ data [65, 66, 69]. The O_h^1-D_{4h}^{18} transition in $SrTiO_3$ and in $KMnF_3$ results from an R point instability of an F_{2u} symmetry phonon whose eigenvector consists of a staggered rotation of anion octahedra about (001) axis, and gives rise to Raman active phonons $A_{1g} + 2\,B_{1g} + 2\,B_{2g} + 3\,E_g$. For a (100) cut crystal the diagonal spectrum contains the A_{1g} and B_{1g} modes and the nondiagonal spectrum contains B_{2g} and E_g modes. In $RbCaF_3$ all these modes except for one in the diagonal spectrum have been identified [66]. The low frequency temperature-dependent modes can be assigned to the A_{1g} and E_g components of an F_{2u} zone boundary soft mode.

For $RbCaF_3$ it is possible, using group theoretical considerations, and the available experimental data, to make a tentative assignment of the space group, D_{4h}^{18}, below the 198 K transition temperature. The Raman data and the tetragonal splitting in the EPR spectrum below 200 K are consistent with an O_h^1-D_{4h}^{18} phase transition driven by an R-point mode [66].

In contrast to the cubic-to-tetragonal phase transitions which seem to have only a small effect on the thermal conductivities, it has been found that the low temperature structural phase transitions produce a strong reduction in the thermal conductivities of $KMnF_3$ and $RbCaF_3$ [69]. The structural phase transition in $LaAlO_3$ around 489 °C [51, 52] belongs to the case when the condensing phonon mode is at the corner R = (1, 1, 1) π/a of the Brillouin zone in the cubic phase. The triply degenerate phonon mode has the R_{25} irreducible representation, i.e. Γ_{25} at the zone centre, and its components can be thought of as alternate librations of the AlO_6 octahedra around the cubic axis. The low temperature phase is rhombohedral D_{3d}^6(R3c) and the distortion from cubic symmetry corresponds to a condensation of a linear combination of all three cubic components of the R_{25} mode. The tetragonal distortion in the $SrTiO_3$ and $KMnF_3$ results from the condensation of only one of the cubic components of the R_{25} mode [52].

Uwe and Sakudo [70-73] studied by dielectric measurements and Raman-scattering experiment the uniaxial stress dependence of the ferroelectric and structural phonon mode transition in $SrTiO_3$ and $KTaO_3$. Anticrossing between the ferroelectric and the structural soft modes was observed for an oblique wave-vector phonon. An anomalous increase of the damping of the totally symmetric ferroelectric mode near the critical stress for the transition has been found. Stress induced ferroelectricity was also investigated in $KTaO_3$ [73-75].

Analysing the ferroelectric modes in $SrTiO_3$ and $KTaO_3$ Migoni *et al.* [76] argued that the strong Raman scattering and the behaviour of the ferroelectric soft mode in oxidic perovskites of the type ABO_3 originate from the unusual anisotropic polarizability of oxygen, enhanced, especially dynamically, by the hybridization of the oxygen p states with the d states of the transition metal ion B in the perovskite.

The lattice normal modes in the cubic perovskite $BaTiO_3$, in the ferroelectric system $Pb_{1-x}Ba_xTiO_3$ and in the ferroelectric tetragonal and perovskite $PbTiO_3$ were measured by the Raman spectroscopy technique below and above the ferroelectric transition temperature T_c [77, 78]. $BaTiO_3$ and, in particular, $PbTiO_3$ is a good example of a ferroelectric below T_c in terms of the lattice modes. The modes obey the appropriate Raman selection rules; the modes are overdamped in $BaTiO_3$ and are underdamped up to T_c in $PbTiO_3$; the modes in $PbTiO_3$ disappear abruptly at T_c when the crystal becomes centrosymmetric, as they should according to selection rules [77, 78].

Optical excitation by laser radiation of ferroelectric $BaTiO_3$ has been investigated by Chanussot [79, 80] : the electron-phonon coupling can give rise to a ferroelectric phase transition via the Jahn-Teller effect.

The densities of valence states in $SrTiO_3$ and $BaTiO_3$ have been investigated by high resolution X-ray photoelectron studies [81].

Cluster surface states of $SrTiO_3$ and $BaTiO_3$ have been calculated [82].

Isotropic $RbMnF_3$ is a nearly ideal Heisenberg antiferromagnet. Its thermal conductivity has been measured [83], a phase diagram has been proposed, tests of scaling and some renormalization group calculations have been done [84].

Precise magnetic measurements of the paramagnetic susceptibility in intense static magnetic fields, and the neutron diffraction and Mössbauer effect studies have been performed in the perovskite type crystal Mn_3SnN [85]. Three first-order transitions and one second-order transition occur and four different crystallographic phases, magnetically ordered, have been observed and found to depend critically on the existence of singularities in the electronic density of states [86].

Superconductivity has been observed in several perovskite compounds. In particular the Zr-doped $SrTiO_3$ is a superconducting semiconductor, with a large penetration depth because of the small carrier concentration. A theoretical model involving screened electron-electron interactions via intervalley optical phonons was applied to fit the transition temperature data [87]. Superconductivity has been observed in a number of degenerate semiconductors such as $SrTiO_{3-x}$ [88], $Sr_{1-y}Ba_yTiO_{3-x}$ [89], etc.

Appel [90] considered the mechanism of the soft mode superconductivity in $SrTiO_{3-x}$ to calculate the transition temperature as a function of the electron concentration.

4. **Theoretical work on perovskites.** — A theoretical examination of the electronic energy bands of cubic strontium titanate has been performed by a semi-empirical L.C.A.O. (linear combination of atomic orbitals) method [91]. In cubic strontium and barium titanates there are six lowest conduction band ellipsoids lying along the (100) axes with the minima located at or near the Brillouin zone boundaries. Characteristic extrema at the zone centre correspond to the forbidden energy gap $\Gamma_{25'}$-Γ_{15}. Apart from the minimum of the conduction band at the zone centre there exist well shaped valleys at the symmetry points X. Energy positions of the $\Gamma_{25'}$ and the X_3 valley are very close and in the doped $SrTiO_3$ all these valleys are populated by electrons. Thus intervalley scattering is possible. Symmetries of the electron and phonon states in the scattering processes are restricted by the selection rules.

Electronic band structures have been calculated by the nonrelativistic augmented-plane-wave method and the tight-binding interpolation scheme for the similar to perovskite ReO_3 compound [92, 93] and for the cubic perovskite-type compounds $KNiF_3$, $SrTiO_3$ [94], $KMoO_3$, and $KTaO_3$ [95, 96] and $BaTiO_3$ [97].

The ferroelectric phase transitions have been extensively studied from the viewpoint of lattice dynamics since the initial theoretical papers by Anderson [98] and Cochran [99]. The soft phonon mode theory is a particularly suitable explanation of ferroelectricity in displacive-type ferroelectrics such as $BaTiO_3$. In $BaTiO_3$, $KTaO_3$, $KNbO_3$ the soft mode is at the zone centre, in $SrTiO_3$, $KMnF_3$ and $LaAlO_3$ at the R point [46, 51, 52].

Phase transitions have been theoretically investigated for $KTaO_3$ and $SrTiO_3$ [73, 44, 95]. Aleksandrov *et al.* [100] have applied the Landau theory of second order phase transitions to calculate possible symmetries resulting from the O_h^1 symmetry and have found as one possible symmetry, after the phase transition, the tetragonal nonsymmorphic space group D_{4h}^{18}. The irreducible small representations for the four space groups D_{4h}^{17} to D_{4h}^{20} based on the bodycentred tetragonal lattice can be read off from the representations of the point groups of the wave vector groups given in tables T 2, 10, 16, 30, 68, 107, 110, 118, 119, 126, 127, 146, 147, 166, 168, 175, 184 and P with the same indices, of Kovalev [9], and small representations for the symmetry points, lines and planes can be found in the paper by Sek [101] where, however, in table 3 the numbering of the tables has to be corrected by adding 3 to the printed table numbers.

5. **Selection rules.** — Selection rules are useful in the investigation of the electron band symmetries, optical transitions, infrared lattice absorption, electron scattering and tunnelling, neutron scattering, magnon side bands, Brillouin scattering, Raman scattering, etc. [102]. Analysis of scattering processes involving photons, phonons or magnons in crystalline solids generally requires the appropriate selection rules to be worked out. Recently attention has been directed to the calculations of the Clebsch-Gordan coefficients of the space group representations [103-110], Birman *et al.* [107-110] have shown that the elements of the first order, one excitation, scattering tensor are precisely certain Clebsch-Gordan coefficients or prescribed linear combinations ; the elements of the second order, two-excitation process are a particular sum of products of Clebsch-Gordan coefficients.

The factorisation of a matrix element or a scattering tensor element into a Clebsch-Gordan coefficient and a reduced matrix element yields a maximum realization of the simplifications from to the symmetry of a problem.

The Clebsch-Gordan coefficients for the irreducible representations of the crystal space groups or the crystal point groups are useful in analysis of the Brillouin scattering tensor, scattering tensors for morphic effects, two photon absorption matrix elements, scattering tensors for multipole-dipole resonance Raman scattering, higher order moment expansions in infrared absorption, and diagonalization of the dynamical matrix of crystal vibrations. For a calculation of the Clebsch-Gordan coefficients or scattering tensors an elaboration of the selection rules is a first necessary step. In fact, a reduction of products of the irreducible representations of the revelant crystal group gives the frequency of occurence of each irreducible representation in a product and thus a survey of the matrix elements which vanish by symmetry alone and of those remaining for which the calculation of the Clebsch-Gordan coefficients is required.

Birman *et al.* [110] have shown that in the effective Hamiltonian matrix each element is a prescribed sum of symmetry adapted components of the Hamiltonian operator times a Clebsch-Gordan coefficient.

6. **Decomposition formula.** — The transition amplitude of an electron from the state $\Psi_q^{\mathbf{m}}$ to the state $\Psi_r^{\mathbf{h}}$ due to an interaction described by the operator $\Psi_p^{\mathbf{k}}$ is proportional to the integral

$$\int \Psi_r^{\mathbf{h}*}(\mathbf{x})\, \Psi_p^{\mathbf{k}}(\mathbf{x})\, \Psi_q^{\mathbf{m}}(\mathbf{x})\, \mathrm{d}^3x\,. \tag{1}$$

The integral vanishes unless the representation $D_r^{\mathbf{h}}$ is contained in the product $D_p^{\mathbf{k}} \times D_q^{\mathbf{m}}$. Thus the selection rules are obtained from decomposition of the Kronecker product of two irreducible representations into irreducible ones

$$D_p^{\mathbf{k}} \times D_q^{\mathbf{m}} = \sum_{\mathbf{h},r} C_{pq,r}^{\mathbf{km},\mathbf{h}}\, D_r^{\mathbf{h}}\,. \tag{2}$$

The irreducible representations are labelled by the wave vectors $\mathbf{k}, \mathbf{m}, \mathbf{h}$ and the indices p, q, r, respectively. The frequency of occurrence $C_{pq,r}^{\mathbf{km},\mathbf{h}}$ of the representation $D_p^{\mathbf{h}}$ in $D_p^{\mathbf{k}} \times D_q^{\mathbf{m}}$ can be expressed in terms of the characters $\psi_p^{\mathbf{k}}$ of the small representations $d_p^{\mathbf{k}}$ which induce the representations $D_p^{\mathbf{k}}$ of the space groups G [111] :

$$C_{pq,r}^{\mathbf{km},\mathbf{h}} = \sum_{\alpha} \frac{1}{|\,\overline{\mathrm{L}}_\alpha\,|} \times$$
$$\times \sum_{S \in \mathrm{L}_\alpha} \psi_{\alpha p}^{\mathbf{k}}(\{ S \mid \tau_s \})\, \psi_{\beta(\alpha)q}^{\mathbf{m}}(\{ S \mid \tau_s \})\, \psi_r^{\mathbf{h}*}(\{ S \mid \tau_s \})\,. \tag{3}$$

Here the sum indexed by α is taken over the revelant leading wave vector selection rules L.W.V.S.R., see Lewis [111], i.e. over the elements determined by the expansion of the point group $\overline{\mathrm{G}}$ into double cosets [8, 111], $\overline{\mathrm{G}} = \sum_\alpha \overline{\mathrm{G}}^{\mathbf{h}}\, \alpha \overline{\mathrm{G}}^{\mathbf{k}}$, where $\overline{\mathrm{G}}^{\mathbf{h}}$ is the point group of the wave vector group $\mathrm{G}^{\mathbf{h}}$ of $\mathbf{h}$ and $\overline{\mathrm{G}}^{\mathbf{k}}$ is the point group of $\mathrm{G}^{\mathbf{k}}$. The index $\beta(\alpha)$ means that β is dependent on α : it is an arbitrary element of $\overline{\mathrm{G}}$ satisfying

$$\alpha\mathbf{k} + \beta\mathbf{m} = \mathbf{h}\,, \tag{4}$$

where $=$ means equality modulo a vector of the reciprocal lattice of the group G. The symbol Σ' is to remind that, if for given $\mathbf{k}, \mathbf{m}, \mathbf{h}$ and α no element β of $\overline{\mathrm{G}}$ satisfying eq. (4) exists, then we have zero instead of the sum over S. $\overline{\mathrm{L}}_\alpha$ is the point group of $\mathrm{L}_\alpha = \mathrm{G}^{\alpha\mathbf{k}} \wedge \mathrm{G}^{\mathbf{h}}$, the intersection of the group $\mathrm{G}^{\alpha\mathbf{k}}$ of the vector $\alpha\mathbf{k}$ and the group $\mathrm{G}^{\mathbf{h}}$ of $\mathbf{h}$. In the symmorphic space group O_h^1 the $\psi_{\alpha p}^{\mathbf{k}}$ and $\psi_{\beta q}^{\mathbf{m}}$ are given by the relations of the type

$$\psi_{\alpha p}^{\mathbf{k}}(S) = \psi_p^{\mathbf{k}}(\alpha^{-1} S \alpha)\,. \tag{5}$$

For the small representation $d_p^{\mathbf{k}}$ of the unbarred primitive translation $\{ E \mid \mathbf{t} \}$ we assume the convention

$$d_p^{\mathbf{k}}(\{ E \mid \mathbf{t} \}) = \hat{1} \exp(+\, i\mathbf{k}\mathbf{t}) \tag{6}$$

i.e. we choose the $+$ sign in the exponent on the right-hand side. $\hat{1}$ is the unit matrix of dimension of the representation $d_p^{\mathbf{k}}$. In the above considerations $\overline{\mathrm{G}}$ can be a single or a double space group. Correspondingly all the groups considered, except G, are single groups or double groups, respectively. If G is a double space group, we use the same symbols for the point operations of a double group as for corresponding operations of the single group. For given $\mathbf{k}$, $\mathbf{m}$ from the representation domain Φ all the vectors $\mathbf{h}$ for which the coefficient (3) may be different from zero can be found as follows : we consider the vectors $\mathbf{k}_i$ from the star of $\mathbf{k}$ and $\mathbf{m}_j$ from the star of $\mathbf{m}$. We construct the vectors $\mathbf{k}_i + \mathbf{m}_j$ with one of the vectors $\mathbf{k}_i$, $\mathbf{m}_j$ fixed and the second varied. In this way, on account of eq. (4), we obtain representants $\mathbf{h} = \mathbf{k}_i + \mathbf{m}_j$ of the star of the vector $\mathbf{h}$ for which the coefficient (3) may be nonvanishing [112-115].

Recently Cracknell and Davies have written two Algol programs, one to determine the wave vector selection rules [116], the other for determining the reductions of the Kronecker products of the irreducible representations of crystallographic space groups [117].

7. **Description of tables.** — We give in table I the coordinates of the symmetry points of the representation domain in the cubic Brillouin zone of the O_h^1-perovskite, O_h^2, O_h^3-beta-wolfram, and O_h^4-cuprite structure.

In table II we list the leading wave vector selection rules, L.W.V.S.R. [111], $\alpha\mathbf{k} + \beta\mathbf{m} = \mathbf{h}$, and intersections

$$\mathrm{N} = \mathrm{G}^{\alpha\mathbf{k}} \wedge \mathrm{G}^{\beta\mathbf{m}} \wedge \mathrm{G}^{\mathbf{h}} = (\alpha \mathrm{G}^{\mathbf{k}} \alpha^{-1}) \wedge (\beta \mathrm{G}^{\mathbf{m}} \beta^{-1}) \wedge \mathrm{G}^{\mathbf{h}} \tag{7}$$

TABLE I

The symmetry points

Point	$\mathbf{k}$
Γ	$(0, 0, 0)\ \pi/a$
R	$(1, 1, 1)\ \pi/a$
M	$(1, 1, 0)\ \pi/a$
X	$(0, 1, 0)\ \pi/a$

TABLE II

Leading wave vector selection rules, L.W.V.S.R., *and intersections*, N *for* O_h^1-O_h^4

L.W.V.S.R.	Intersections
$\alpha\mathbf{k} + \beta\mathbf{m} = \mathbf{h}$	$N = G^{\alpha\mathbf{k}} \wedge G^{\beta\mathbf{m}} \wedge G^{\mathbf{h}}$
$\mathbf{k}_\Gamma + \mathbf{k}_\Gamma = \mathbf{k}_\Gamma$	$G^{\mathbf{k}_\Gamma}$
$\mathbf{k}_\Gamma + \mathbf{k}_R = \mathbf{k}_R$	$G^{\mathbf{k}_\Gamma}$
$\mathbf{k}_\Gamma + \mathbf{k}_M = \mathbf{k}_M$	$G^{\mathbf{k}_M}$
$\mathbf{k}_\Gamma + \mathbf{k}_X = \mathbf{k}_X$	$G^{\mathbf{k}_X}$
$\mathbf{k}_R + \mathbf{k}_R = \mathbf{k}_\Gamma$	$G^{\mathbf{k}_\Gamma}$
$\mathbf{k}_R + 5\ \mathbf{k}_M = \mathbf{k}_X$	$G^{\mathbf{k}_X}$
$\mathbf{k}_R + 9\ \mathbf{k}_X = \mathbf{k}_M$	$G^{\mathbf{k}_M}$
$\mathbf{k}_M + \mathbf{k}_M = \mathbf{k}_\Gamma$	$G^{\mathbf{k}_M}$
$5\ \mathbf{k}_M + 9\ \mathbf{k}_M = \mathbf{k}_M$	$N = \{1, 2, 3, 4, 25, 26, 27, 28\}$
$\mathbf{k}_M + 9\ \mathbf{k}_X = \mathbf{k}_R$	$G^{\mathbf{k}_M}$
$\mathbf{k}_M + 5\ \mathbf{k}_X = \mathbf{k}_X$	$N = \{1, 2, 3, 4, 25, 26, 27, 28\}$
$\mathbf{k}_X + \mathbf{k}_X = \mathbf{k}_\Gamma$	$G^{\mathbf{k}_X}$
$\mathbf{k}_X + 5\ \mathbf{k}_X = \mathbf{k}_M$	$N = \{1, 2, 3, 4, 25, 26, 27, 28\}$

of the wave vector groups $G^{\alpha\mathbf{k}}$, $G^{\beta\mathbf{m}}$ and $G^{\mathbf{h}}$, see eq. (4). For instance, the wave vector selection rule $\mathbf{k}_R + 5\ \mathbf{k}_M = \mathbf{k}_X$ means that $\mathbf{k}_R + h_5\ \mathbf{k}_M = \mathbf{k}_X$ modulo a vector of the reciprocal lattice, where h_5 is the operation numbered 5 in the table I of M-L [4], p. 123. The $N = G^{\mathbf{k}_X}$ is the intersection of the three wave vector groups of the vectors $\mathbf{k}_R$, $5\ \mathbf{k}_M$ and $\mathbf{k}_X$, i.e. $G^{\mathbf{k}_R} \wedge G^{5\mathbf{k}_M} \wedge G^{\mathbf{k}_X}$. For the L.W.V.S.R.

$$5\ \mathbf{k}_M + 9\ \mathbf{k}_M = \mathbf{k}_M$$

the intersection N consists of space operations 1, 2, 3, 4, 25, 26, 27, 28 of M-L. Notice that these wave vector selection rules apply equally to all crystal symmetries with space groups O_h^1, O_h^2, O_h^3 and O_h^4.

In tables III, IV and V we give the decompositions of the Kronecker products of the irreducible representations of the space group O_h^1 into irreducible representations, according to eq. (2) where $\mathbf{k}$ and $\mathbf{m}$ are vectors to the four high symmetry points of the Brillouin zone.

In table III it is understood that the selection rules for $\Gamma \times R$ are obtained from those of $\Gamma \times \Gamma$ by substituting in the left-hand side for the second factor Γ_j the corresponding factor R_j and in the right-hand side for Γ_k the corresponding R_k. As can be seen from the character tables, the equality

$$\Gamma_i \times R_j = \Gamma_j \times R_i$$

holds, thus for the decomposition of $\Gamma \times R$ there is no need to write out the empty part of table III. Similarly $M_i \times X_j = M_j \times X_i$ in table V. The decompositions of $R \times R$ are obtained from those of $\Gamma \times \Gamma$ by substituting in the left-hand side $\Gamma \to R$. Similar substitutions will do for the selection rules in table IV and table V. We present also the decompositions of the Kronecker squares $D_p^{\mathbf{k}} \times D_p^{\mathbf{k}}$ of the irreducible representations of the group into symmetrized and antisymmetrized squares, $[D_p^{\mathbf{k}}]_+^2$ and $[D_p^{\mathbf{k}}]_-^2$, respectively [111]. We do this by writing in the tables the labels of irreducible representations $D_r^{\mathbf{h}}$ appearing in the decomposition of $[D_p^{\mathbf{k}}]_+^2$ in square brackets. In the tables the irreducible representations of the group O_h^1 are labelled by the Miller and Love [4] labels of the corresponding small representations, numbers in position of power exponents mean frequency of occurence c_i of the given irreducible representation. In table VI we summarize the notations of the single valued and the double valued representations according to BSWE [5, 6], Kovalev [9] and M-L [4] for the points Γ and R and in table VII for the single valued representations for the points M and X.

8. **Applications.** — One of the most important applications of the selection rules concern the photon-

TABLE III

$\Gamma \times \Gamma = \Gamma_- \times \Gamma_- = \sum c_i \Gamma_i$, $\Gamma_- \times \Gamma = \sum c_i \Gamma_{i-}$, $R \times R = R_- \times R_- = \sum c_i \Gamma_i$, $R_- \times R = \sum c_i \Gamma_{i-}$,

$\Gamma \times R = \Gamma_- \times R_- = \sum c_i R_i$, $\Gamma_- \times R = \Gamma \times R_- = \sum c_i R_{i-}$,

	Γ_1	Γ_2	Γ_3	Γ_4	Γ_5	Γ_6	Γ_7	Γ_8
Γ_1	[1]	2	3	4	5	6	7	8
Γ_2		[1]	3	5	4	7	6	8
Γ_3			[13] 2	45	45	8	8	678
Γ_4				[135] 4	2 345	68	78	678^2
Γ_5					[135] 4	78	68	678^2
Γ_6						[4] 1	25	345
Γ_7							[4] 1	345
Γ_8								$[24^2\ 5]$ 135

Table IV

$$\Gamma \times M = \Gamma_- \times M_- = \sum c_i M_i, \qquad \Gamma_- \times M = \Gamma \times M_- = \sum c_i M_{i-},$$
$$\Gamma \times X = \Gamma_- \times X_- = \sum c_i X_i, \qquad \Gamma_- \times X = \Gamma \times X_- = \sum c_i X_{i-},$$
$$R \times M = R_- \times M_- = \sum c_i X_i, \qquad R_- \times M = R \times M_- = \sum c_i X_{i-},$$
$$R \times X = R_- \times X_- = \sum c_i M_i, \qquad R_- \times X = R \times X_- = \sum c_i M_{i-},$$

		X_1	X_2	X_3	X_4	X_5	X_6	X_7		
		M_1	M_2	M_3	M_4	M_5	M_6	M_7		
Γ_1	Γ_1	1	2	3	4	5	6	7	R_1	R_1
Γ_2	Γ_2	2	1	4	3	5	7	6	R_2	R_2
Γ_3	Γ_3	12	12	34	34	5^2	67	67	R_3	R_3
Γ_4	Γ_4	35	45	15	25	12 345	$6^2 7$	67^2	R_4	R_4
Γ_5	Γ_5	45	35	25	15	12 345	67^2	$6^2 7$	R_5	R_5
Γ_7	Γ_6	6	7	6	7	67	135	245	R_7	R_6
Γ_6	Γ_7	7	6	7	6	67	245	135	R_6	R_7
Γ_8	Γ_8	67	67	67	67	$6^2 7^2$	$12\ 345^2$	$12\ 345^2$	R_8	R_8
		M_1	M_2	M_3	M_4	M_5	M_7	M_6		
		X_1	X_2	X_3	X_4	X_5	X_7	X_6		

Table V

$$M \times M = M_- \times M_- = \sum c_i \Gamma_i + \sum c_j M_j, \qquad M_- \times M_+ = \sum c_i \Gamma_{i-} + \sum c_j M_{j-},$$
$$X \times X = X_- \times X_- = \sum c_i \Gamma_i + \sum c_j M_j, \qquad X_- \times X_+ = \sum c_i \Gamma_{i-} + \sum c_j M_{j-},$$
$$M \times X = M_- \times X_- = \sum c_i R_i + \sum c_j X_j, \qquad M \times X_- = M_- \times X = \sum c_i R_{i-} + \sum c_j X_{j-},$$

	M_1		M_2		M_3		M_4		M_5		M_6		M_7		
	Γ	M	Γ	M	Γ	M	Γ	M	Γ	M	Γ	M	Γ	M	
M_1	[13]	[1] 2	23	12	4	5	5	5	45	345	68	67	78	67	X_1
M_2			[13]	[1] 2	5	5	4	5	45	345	78	67	68	67	X_2
M_3					[13]	[4] 3	23	34	45	125	68	67	78	67	X_3
M_4							[13]	[4] 3	45	125	78	67	68	67	X_4
M_5									$[123^2\ 5]\ 4$	[145] 235	678^2	$6^2\ 7^2$	678^2	$6^2\ 7^2$	X_5
M_6											$[4^2\ 5]\ 13$	[145] 235	$2\ 345^2$	$12\ 345^2$	X_7
M_7													$[4^2\ 5]\ 13$	[145] 235	X_6
	R	X	R	X	R	X	R	X	R	X	R	X	R	X	
	X_1		X_2		X_3		X_4		X_5		X_7		X_6		

Table VI

Labels of the irreducible representations for the points Γ and R in O_h^1

Miller, Love [4] p. 393, 394	Kovalev [9] p. 92	Bouckaert, Smoluchowski, Wigner [5]	Elliott [6]
—	—	—	—
GM 1 +	T 205 τ_1	Γ_1	Γ_{1+}
2 +	τ_2	Γ_2	Γ_{2+}
3 +	τ_3	Γ_{12}	Γ_{12+}
4 +	τ_5	Γ_{15}'	Γ_{15+}
5 +	τ_4	Γ_{25}'	Γ_{25+}
1 −	τ_6	Γ_1'	Γ_{1-}
2 −	τ_7	Γ_2'	Γ_{2-}
3 −	τ_8	Γ_{12}'	Γ_{12-}
4 −	τ_{10}	Γ_{15}	Γ_{15-}
5 −	τ_9	Γ_{25}	Γ_{25-}
6 +	P 205 π_2		Γ_{6+}
7 +	π_1		Γ_{7+}
8 +	π_3		Γ_{8+}
6 −	π_5		Γ_{7-}
7 −	π_4		Γ_{6-}
8 −	π_6		Γ_{8-}

Table VII

Labels of the irreducible representations for the points M and X in O_h^1

Miller, Love [4] p. 394		Kovalev [9] p. 80, 92 T 147		Bouckaert, Smoluchowski, Wigner [5], Elliott [6]	
—		—		—	
M	X	M	X	M	X
1 +	1 +	τ_1	τ_1	M_1	X_1
2 +	2 +	τ_5	τ_5	M_2	X_2
3 +	3 +	τ_3	τ_3	M_4	X_4
4 +	4 +	τ_7	τ_7	M_3	X_3
5 +	5 +	τ_9	τ_9	M_5	X_5
1 −	1 −	τ_2	τ_2	M_1'	X_1'
2 −	2 −	τ_6	τ_6	M_2'	X_2'
3 −	3 −	τ_4	τ_4	M_4'	X_4'
4 −	4 −	τ_8	τ_8	M_3'	X_3'
5 −	5 −	τ_{10}	τ_{10}	M_5'	X_5'
6 +	6 +			M_{6+}	
7 +	7 +			M_{7+}	
6 −	6 −			M_{6-}	
7 −	7 −			M_{7-}	

and phonon-involving electronic transitions. The matrix element for the interaction between a conduction electron in state $\mathbf{k}$ and a phonon with wave vector $\mathbf{q}$ and branch index j is given in accordance with eq. (1) by

$$g^0(\mathbf{q}\,j) = \int_{\text{crystal}} \Psi^*_{\mathbf{k}+\mathbf{q}}\, H_{\text{pert}}(\mathbf{q}\,j)\, \Psi_{\mathbf{k}}\, d^3x. \quad (8)$$

The matrix element $g^0(\mathbf{q}\,j)$ is different from zero if the inner Kronecker product of the representation of $\Psi_{\mathbf{k}+\mathbf{q}}$ and $\Psi_{\mathbf{k}}$ contains the representation according to which H_{pert} transforms [90]. Therefore the selection rules determine matrix elements which vanish by symmetry alone.

In the special case $\mathbf{q} = 0$, the matrix element is finite, if the symmetric Kronecker product between the representations of $\Psi_{\mathbf{k}}$ contains the $\mathbf{q} = 0$ phonon symmetry. The symmetry of the $\mathbf{q} = 0$ displacement field is higher than that for any finite $\mathbf{q}$. Consequently, if the matrix element is finite for $\mathbf{q} = 0$, it will also be finite near $\mathbf{q} = 0$.

It is to be stressed that for high symmetry like O_h^1 there appear many selections rules which are particularly simple in the sense that the decomposition of direct product of irreducible representations consists of only one irreducible representation. Examples can be seen in tables III-V. Referring to the intervalley scattering between $\Gamma_{25'}$ and X_3 conduction band minima, in $SrTiO_3$, mentioned in section 4, we read from table IV and table VI, VII the decomposition $\Gamma_{25'} \times X_3 = X_1 + X_5$ in the notation of BSW [5]. Therefore the phonons in the intervalley scattering between the $\Gamma_{25'}$ and X_3 minima can be of the symmetry X_1 and X_5.

Appendix. — Dr. A. P. Cracknell has kindly pointed out to us, from the output of his programs [116, 117], the misprints in our published selection rules for the beta-wolfram structure [114]. The correct entries in table III of [114] read

$$\Gamma_1^- \times R_2 = R_3\,, \quad \Gamma_1^- \times R_3 = R_2\,,$$
$$\Gamma_2^- \times R_2 = R_3\,, \quad \Gamma_2^- \times R_3 = R_2\,,$$
$$\Gamma_1^- \times R_6 = R_7\,, \quad \Gamma_1^- \times R_7 = R_6\,,$$
$$\Gamma_2^- \times R_6 = R_7\,, \quad \Gamma_2^- \times R_7 = R_6\,.$$

In table XI of [114], for $i = 1, 2, 3, 4$,

$$X_i \times X_5 = \Gamma\, 6 7 \bar{6} \bar{7} 8^2\, \bar{8}^2 + M 6^2\, 7^2\, \bar{6}^2\, \bar{7}^2\,.$$

We also thank Drs. A. P. Cracknell and B. L. Davies for their output of the computer program for reduction of the Kronecker products of the irreducible representations for the O_h^1 space group which allowed us a visual check of our tables.

References

[1] SLATER, J. C., Quarterly Progress Report, Solid-State and Molecular Theory Group, *M.I.T.* **46** (1962) 6.
[2] SLATER, J. C., Quarterly Progress Report, Solid-State and Molecular Theory Group, *M.I.T.* **47** (1963) 54.
[3] BEAMER, W. H. and MAXWELL, L. R., *J. Chem. Phys.* **17** (1949) 1288, 1293.
[4] MILLER, S. C. and LOVE, W. F., *Tables of Irreducible Representations of Space Groups and Co-Representations of Magnetic Space Groups* (Pruett Press, Boulder, Colorado) 1967.
[5] BOUCKAERT, L. P., SMOLUCHOWSKI, R. and WIGNER, E., *Phys. Rev.* **50** (1936) 58.
[6] ELLIOTT, R. J., *Phys. Rev.* **96** (1954) 266, 280.
[7] ZAK, J., CASHER, A., GLÜCK, M. and GUR, Y., *The Irreducible Representations of Space Groups* (W. A. Benjamin, Inc., New York) 1969.
[8] BRADLEY, C. J. and CRACKNELL, A. P., *The Mathematical Theory of Symmetry in Solids* (Clarendon Press, Oxford) 1972.
[9] KOVALEV, O. V., *Irreducible Representations of the Space Groups*, Kiev 1961 (in Russian).
[10] TOVSTYUK, K. D. and TARNAVSKAYA, M. V., *Fiz. Tver. Tel.* **5** (1963) 815; *Soviet Solid State Phys.* **5** (1963) 597.
[11] LYNCH, D. W., *Phys. Rev.* **127** (1962) 1537.
[12] HENRY, C. H., SCHNATTERLY, S. E. and SLICHTER, C. P., *Phys. Rev.* **137** (1965) A 583.
[13] SUFFCZYNSKI, M., *J. Chem. Phys.* **38** (1963) 1558.
[14] SMITH, D. Y., *Phys. Rev.* **137** (1965) A 574.
[15] MORAN, P. R., *Phys. Rev.* **137** (1965) A 1016.
[16] ONODERA, Y., *J. Phys. Soc. Jpn* **25** (1968) 469.
[17] INOUE, M. and OKAZAKI, M., *J. Phys. Soc. Jpn* **31** (1971) 1313.
[18] OVERHOF, H. and TREUSCH, J., *Solid State Commun.* **9** (1971) 53.
[19] OVERTON, J. and HERNANDEZ, J. P., *Phys. Rev. B* **7** (1973) 778.
[20] LIN, S. F. and SPICER, W. E., *Phys. Rev. B* **14** (1976) 4559.
[21] BACHRACH, R. Z. and BROWN, F. C., *Phys. Rev. B* **1** (1970) 818.
[22] MOHLER, E., SCHLÖGL, G. and TREUSCH, J., *Phys. Rev. Lett.* **27** (1971) 424.
[23] TREUSCH, J., *Phys. Rev. Lett.* **34** (1975) 1343.
[24] UIHLEIN, Ch. and TREUSCH, J., *Solid State Commun.* **17** (1975) 685.
[25] DISTEFANO, T. H., *Phys. Rev. B* **7** (1973) 1565.
[26] BATES, Jr., C. W., SALAU, A. and LENIART, D., *Phys. Rev. B* **15** (1977) 5963.
[27] HSU, O. L. and BATES, Jr., C. W., *Phys. Rev. B* **15** (1977) 5821.
[28] RÖSELER, U., *Phys. status solidi* (b) **34** (1969) 207.
[29] KURITA, S. and KOBAYASHI, K., *J. Phys. Soc. Jpn* **30** (1971) 1645.
[30] KURITA, S., KOBAYASHI, K. and ONODERA, Y., *Prog. Theor. Phys.* Suppl. **57** (1975) 10.
[31] KONDO, S., NAKAMURA, K., FUJITA, M. and NAKAI, Y., *J. Phys. Soc. Jpn* **38** (1975) 1400.
[32] NAKAMURA, K., FUJITA, M., OHNO, N., KONDO, S. and NAKAI, Y., *J. Phys. Soc. Jpn* **41** (1976) 1636.
[33] INOUYE, C. S. and PONG, W., *Phys. Rev. B* **15** (1977) 2265.
[34] HAQUE, M. S. and STRAUCH, D., *Phys. Rev. B* **15** (1977) 5898.
[35] KNOX, R. S., SHULMAN, R. G. and SUGANO, S., *Phys. Rev.* **130** (1963) 512.
[36] SHULMAN, R. G. and SUGANO, S., *Phys. Rev.* **130** (1963) 506.
[37] SUGANO, S. and SHULMAN, R. G., *Phys. Rev.* **130** (1963) 517.
[38] SHIRANE, G. and YAMADA, Y., *Phys. Rev.* **177** (1969) 858.
[39] UNOKI, H. and SAKUDO, T., *J. Phys. Soc. Jpn* **23** (1967) 546.

[40] LYTLE, F. W., *J. Appl. Phys.* **35** (1964) 2212.
[41] RIMAI, L. and DEMARS, G. A., *Phys. Rev.* **127** (1962) 702.
[42] BELL, R. O. and RUPPRECHT, G., *Phys. Rev.* **129** (1963) 90.
[43] FLEURY, P. A., SCOTT, J. F. and WORLOCK, J. M., *Phys. Rev. Lett.* **21** (1968) 16.
[44] COWLEY, R. A., *Phys. Rev.* **134** (1964) A 981.
[45] RISTE, T., SAMUELSON, E. J., OTNES, K. and FEDER, J., *Solid State Commun.* **9** (1971) 1455.
[46] SHAPIRO, S. M., AXE, J. D., SHIRANE, G. and RISTE, T., *Phys. Rev. B* **6** (1972) 4332.
[47] SHIRANE, G., MINKIEWICZ, V. J. and LINZ, A., *Solid State Commun.* **8** (1970) 1941.
[48] MINKIEWICZ, V. J., FUJII, Y. and YAMADA, Y., *J. Phys. Soc. Jpn* **28** (1970) 443.
[49] GESI, K., AXE, J. D., SHIRANE, G. and LINZ, A., *Phys. Rev. B* **5** (1972) 1933.
[50] TÖPLER, J., ALEFELD, B. and HEIDEMANN, A., *J. Phys. C : Solid State Phys.* **10** (1977) 635.
[51] AXE, J. D., SHIRANE, G. and MÜLLER, K. A., *Phys. Rev.* **183** (1969) 820.
[52] KJEMS, J. K., SHIRANE, G., MÜLLER, K. A. and SCHEEL, H. J., *Phys. Rev. B* **8** (1973) 1119.
[53] WILLEMSEN, H. W., ARMSTRONG, H. L. and MEINSCKE, P. P. M., *Phys. Rev. B* **14** (1976) 3644.
[54] YAMADA, Y., SHIRANE, G. and LINZ, A., *Phys. Rev.* **177** (1969) 848.
[55] HARADA, J., AXE, J. D. and SHIRANE, G., *Phys. Rev. B* **4** (1971) 155.
[56] DIDOMENICO Jr., M., WEMPLE, S. H., PORTO, S. P. S. and BAUMAN, R. P., *Phys. Rev.* **174** (1968) 522.
[57] NAKAMURA, T., *Ferroelectrics* **9** (1975) 159.
[58] FLEURY, P. A. and LAZAY, P. D., *Phys. Rev. Lett.* **26** (1971) 1331.
[59] FLEURY, P. A., *Annu. Rev. Mater. Sci.* **6** (1976) 157.
[60] SCOTT, J. F., *Rev. Mod. Phys.* **46** (1974) 83.
[61] HIDAKA, M., *J. Phys. Soc. Jpn* **39** (1975) 180.
[62] STRAUSS, E. and RIEDERER, H. J., *Solid State Commun.* **21** (1977) 429.
[63] BÜRGER, H., STROBEL, K., GEICK, R. and MÜLLER-LIERHEIM, W., *J. Phys. C : Solid State Phys.* **9** (1976) 4213.
[64] STROBEL, K. and GEICK, R., *J. Phys. C : Solid State Phys.* **9** (1976) 4223.
[65] MODINE, F. A., SONDER, E., UNRUH, W. P., FINCH, C. B. and WESTBROOK, R. D., *Phys. Rev. B* **10** (1974) 1623.
[66] RUSHWORTH, A. J. and RYAN, J. F., *Solid State Commun.* **18** (1976) 1239.
[67] ROUSSEAU, M., NOUET, J. and ALMAIRAC, R., *J. Physique* **38** (1977) 1423.
[68] ALMAIRAC, R., ROUSSEAU, M., GESLAND, J. Y., NOUET, J. and HENNION, B., *J. Physique* **38** (1977) 1429.
[69] MARTIN, J. J., DIXON, G. S. and VELASCO, P. P., *Phys. Rev. B* **14** (1976) 2609.
[70] UWE, H. and SAKUDO, T., *J. Phys. Soc. Jpn* **38** (1975) 183.
[71] UWE, H., UNOKI, H., FUJII, Y. and SAKUDO, T., *Solid State Commun.* **13** (1973) 737.
[72] UWE, H. and SAKUDO, T., *Phys. Rev. B* **13** (1976) 271.
[73] UWE, H. and SAKUDO, T., *Phys. Rev. B* **15** (1977) 337.
[74] AXE, J. D., HARADA, J. and SHIRANE, G., *Phys. Rev. B* **1** (1970) 1227.
[75] SAMARA, G. A. and MOROSON, B., *Phys. Rev. B* **8** (1973) 1256.
[76] MIGONI, R., BILZ, H. and BÄUERLE, D., *Phys. Rev. Lett.* **37** (1976) 1155.
[77] BURNS, G. and SCOTT, B. A., *Phys. Rev. B* **7** (1973) 3088.
[78] BURNS, G., *Phys. Rev. B* **10** (1974) 1961.
[79] CHANUSSOT, G. and THIEBAUD, C., *Ferroelectrics* **8** (1974) 665, 671.
[80] CHANUSSOT, G., *Ferroelectrics* **10** (1976) 149.
[81] BATTYE, F. L., HÖCHST, H. and GOLDMANN, A., *Solid State Commun.* **19** (1976) 269.
[82] WOLFRAM, T., HURST, R. and MORIN, F. J., *Phys. Rev. B* **15** (1977) 1151.
[83] AATMAN, J. B., *Phys. Rev. B* **15** (1977) 273.
[84] SHAPIRA, Y. and BECERNA, C. C., *Phys. Rev. Lett.* **38** (1977) 358.
[85] FRUCHART, D., BERTAUT, E. F., SÉNATEUR, J. P. and FRUCHART, R., *J. Physique Lett.* **38** (1977) L-21.
[86] JARDIN, J. P. and LABBÉ, J., *J. Physique* **36** (1975) 1317.
[87] EAGLES, D. M., *Phys. Rev.* **178** (1969) 668.
[88] SCHOOLEY, J. F., HOSLER, W. R. and COHEN, M. L., *Phys. Rev. Lett.* **12** (1964) 474.
[89] SCHOOLEY, J. F., FREDERIKSE, H. P. R., HOSLER, W. R. and PFEIFFER, E. R., *Phys. Rev.* **159** (1967) 301.
[90] APPEL, J., *Phys. Rev.* **180** (1969) 508.
[91] KAHN, A. H. and LEYDENDECKER, A. J., *Phys. Rev.* **135** (1964) A 1321.
[92] MATTHEISS, L. F., *Phys. Rev.* **181** (1969) 987.
[93] MATTHEISS, L. F., *Phys. Rev. B* **2** (1970) 3918.
[94] SOULES, T. F., KELLY, E. J., VAUGHT, D. M. and RICHARDSON, J. M., *Phys. Rev. B* **6** (1872) 1519.
[95] MATTHEISS, L. F., *Phys. Rev. B* **6** (1972) 4718, 4740.
[96] ELLIALTIOGLU, S. and WOLFRAM, T., *Phys. Rev. B* **15** (1977) 5909.
[97] MICHEL-CALENDINI, F. and MESNARD, M. G., *Phys. status solidi* (b) **44** (1971) K 117, *J. Phys. C : Solid State Phys.* **6** (1973) 1709.
[98] ANDERSON, P. W., *Proc. Conf. on the Physics of Dielectrics* (Academy of Sciences, Moscow, 1958), Izd. AN., Moscow 1960, p. 290.
[99] COCHRAN, W., *Adv. Phys.* **9** (1960) 387, **18** (1969) 157.
[100] ALEKSANDROV, K. S., ZINENKO, V. I., MICHELSON, L. M. and SIROTIN, Y. I., *Kristallografiya* **14** (1969) 327.
[101] SEK, Z., *Phys. status solidi* **3** (1963) 2155.
[102] CRACKNELL, A. P., *Adv. Phys.* **23** (1974) 673.
[103] SAKATA, I., *J. Math. Phys.* **15** (1974) 1702, 1710.
[104] BERENSON, R. and BIRMAN, J. L., *J. Math. Phys.* **16** (1975) 227.
[105] BERENSON, R., ITZKAN, I. and BIRMAN, J. L., *J. Math. Phys.* **16** (1975) 236.
[106] SCHINDLER, S. and MIRMAN, R., *J. Math. Phys.* **18** (1977) 1678, 1697.
[107] BIRMAN, J. L. and BERENSON, R., *Phys. Rev. B* **9** (1974) 4512.
[108] BIRMAN, J. L., *Phys. Rev. B* **9** (1974) 4518.
[109] BIRMAN, L. J., *Theory of Crystal Space Groups and Infra-Red and Raman Lattice Processes of Insulating Crystals, in Encyclopedia of Physics*, vol. XXV/2b, Light and Matter Ib (Ed. S. Flügge, Springer-Verlag, Berlin-Heidelberg-New York) 1974.
[110] BIRMAN, J. L., LEE, T.-K. and BERENSON, R., *Phys. Rev. B* **14** (1976) 318.
[111] LEWIS, D. H., *J. Phys. A* **6** (1973) 125.
[112] OLBRYCHSKI, K. and NGUYEN, VAN HUONG, *Acta Phys. Pol. A* **37** (1970) 369.
[113] OLBRYCHSKI, K., KOLODZIEJSKI, R., SUFFCZYNSKI, M. and KUNERT, H., *J. Physique* **36** (1975) 985; **37** (1976) 1483.
[114] NGUYEN VAN HUONG, PHAM DO TIEN, KUNERT, H. and SUFFCZYNSKI, M., *J. Physique* **38** (1977) 51.
[115] CRACKNELL, A. P. and DAVIES, B. L., *J. Phys. C : Solid State Phys.* **10** (1977) 2741.
[116] CRACKNELL, A. P. and DAVIES, B. L., *Group Theory Colloquium*, Tübingen (1977).
[117] DAVIES, B. L. and CRACKNELL, A. P., *Group Theory Colloquium*, Tübingen (1977).